

Silicon Device Processing in H-Ambients: H-Diffusion Mechanisms and Influence on Electronic Properties

BHUSHAN SOPORI,¹ YI ZHANG,^{1,2} and N.M. RAVINDRA²

1.—National Renewable Energy Laboratory, 1617 Cole Boulevard, Golden, CO 80401. 2.—Department of Physics, New Jersey Institute of Technology, 16 Warren Street, Newark, NJ 07102

Hydrogen is an electronically active impurity in Si with some unique properties—it can passivate other impurities and defects, both at the interface and in the bulk. Controlled introduction of H can lower interface state density, and thereby improve Schottky and MOS devices, and can reduce bulk recombination to increase minority-carrier-controlled device performance. However, excess H can also introduce defects that can be detrimental to the device properties. Although H is typically introduced by exposing the device to a flux of atomic species, a suitable device configuration can be passivated by thermal treatment in forming gas. This paper addresses some basic issues of device processing in H ambient to improve device performance.

Key words: Solar cells, hydrogen, passivation, impurities, defects

INTRODUCTION

Recent research has shown that H plays an important role in improving many Si devices whose performance is limited by defects and impurities. Hydrogen saturates dangling bonds at interfaces and at point and extended defects, thereby reducing the carrier recombination and improving device characteristics.^{1,2} For example, hydrogenation of an oxide-passivated N/P junction can reduce the diode leakage current by an order of magnitude.³ The forming gas anneal used in metal-oxide-semiconductor (MOS) device fabrication is known to passivate the dangling bonds at Si-SiO₂ interfaces.⁴ Hydrogen also passivates dangling bonds in a-Si devices.^{5,6} Thus, H dilution of Si-bearing gases is necessary to deposit electronically high-quality amorphous Si (a-Si)⁷ suitable for the fabrication of high-efficiency solar cells. Unfortunately, a-Si gradually degrades by exposure to light through the Staebler-Wronski effect, which seems to stem from H itself.^{8,9} Hydrogen can passivate grain boundaries of polycrystalline Si (poly-Si).^{10,11} Concomitantly, hydrogenation is used in Si solar cells^{12,13} and in thin-film transistor (TFT) applications to passivate grain boundaries in poly-Si.^{14,15} Hydrogen can also interact with impurities in Si. The nature of such interactions depends on the type of impurities. For example, it can deactivate shallow

dopants, both acceptor^{16,17} and donor^{18,19} types, leading to changes in the resistivity of the wafer. Although this effect is an undesirable feature for most cases, it can be used to reversibly alter dopant activity and to form erasable P/N junctions in some future applications. Atomic H can interact with metallic impurities such as Fe,²⁰ Cr,²¹ Ni,²² Cu,²² and Au²³ to reduce their carrier recombination in Si. Hydrogen interactions with O exhibit a very interesting behavior—it appears that H diffusivity is lowered by the O, whereas the diffusivity of O donors is greatly enhanced.^{24,25}

In this paper, we will first review briefly the structure of H in a perfect Si lattice and then extend these concepts to imperfect Si containing defects and impurities. Next, we will discuss hydrogenation methods and defects produced by this process. A review of H diffusion mechanisms in Si will be presented here. An understanding of H diffusion in Si is pivotal to designing suitable processes. Finally, we will discuss the influence of H on device performance. Although H has the potential to improve many devices, only a few are used in commercial device fabrication. Perhaps an improved understanding of the properties of H in Si will help extend the range of applications. This review addresses Si devices in general and solar cells in particular.

NATURE OF HYDROGEN IN SILICON

The behavior of H in Si is complicated by the fact that it readily interacts with the lattice, as well as

with nearly all the impurities and defects in Si. In a perfect Si lattice, H is known to be an interstitial impurity that can influence electrical and optical behavior of Si. However, the solubility (S) of H in the Si lattice is quite low. The early study of solubility of H in c-Si was done by van Wieringen and Warmholtz.²⁶ From high-temperature permeation experiments, they derived the following expression for solubility, S :

$$S = 4.96 \times 10^{21} e^{-\frac{1}{kT}(1.86\text{eV})} \text{ (at./ cm}^3\text{)} \quad (1)$$

Figure 1 is a plot of the solubility of H in Si as a function of temperature. It is seen that at the temperatures typically used for hydrogenation, the solubility of H in the Si lattice is very low. For example, at 400°C, the value of S is only about 10^5 cm^{-3} . At these levels, the effect of H on the properties of Si would be negligible, difficult to measure, and not particularly significant for device applications. Thus, it may appear that a study of interactions of H with the Si lattice is not very fruitful. As will be shown later, the primary mechanism for H diffusion is via lattice interactions. Thus, these processes are important for understanding the diffusion properties of H.

In an imperfect lattice, H can associate with impurities and defects, resulting in two important effects—their deactivation (or passivation) and “trapping” of H. The former mechanism is of great significance for device applications, whereas the latter is crucial in dealing with the diffusion behavior of H. Another effect of trapping is that it leads to a higher H concentration in Si than dictated by the lattice solubility in Eq. 1. This concept of increased “effective solubility” can be applied to explain many unusual phenomena of H in Si. We will summarize salient features of H in a perfect lattice and its interactions with defects and impurities.

Hydrogen in a Perfect Si lattice

The structure of H in a Si lattice has been investigated in some detail through experimental analyses and detailed theory. The experimental substantiation of H in a perfect lattice is scanty because of its

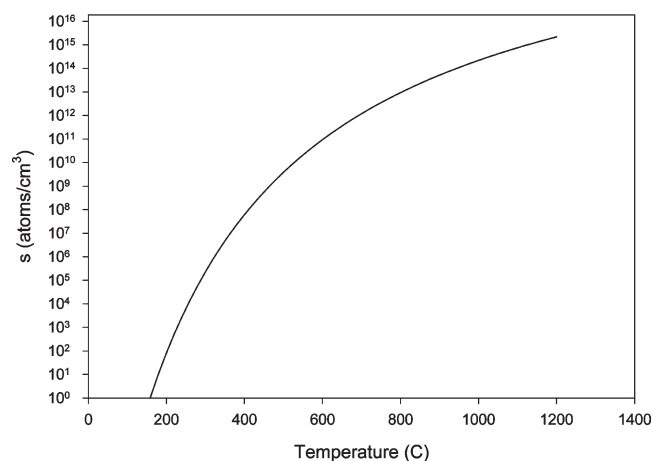


Fig. 1. Solubility of H in Si using Eq. 1.

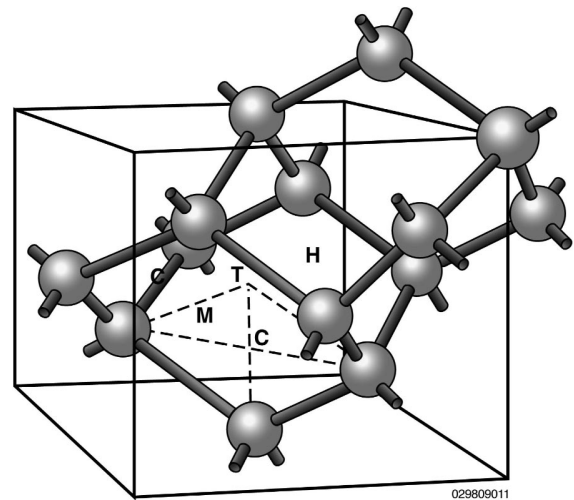


Fig. 2. A sketch of the Si lattice showing important interstitial sites.²⁷

low solubility. Major results have come from early experiments that used channeling and infrared (IR) spectroscopy on H- or D-implanted, high-resistivity Si samples. These measurements have revealed information on the stable sites of H in Si. The sites can be visualized easily by referring to Fig. 2, which is a sketch of a portion of a Si lattice showing the tetrahedral (T), hexagonal (H), and interstitial sites C and M.²⁷ The C site is at the center of the rhombus formed by three adjacent substitutional sites and the nearest T site. An M site is the midpoint between two adjacent C sites.

Initial experiments and theory have yielded very conflicting results. For example, experimental evidence showed that, in deuterium-implanted samples, most of the deuterium was located at 1.6 Å from a Si atom along the $\langle 111 \rangle$ direction. This suggested that H would be located at the antibonding sites. Later work identified that this configuration was related to a vacancy-H complex, and similar problems occurred in theory, too. Early calculations were performed using small cluster sizes (limited by computational capabilities) and implicit assumptions that H would not strongly bond to a crystalline network and would favor interstitial locations where the interactions with the Si charge density would be minimal. These calculations also excluded lattice relaxation. The results obtained by such analyses led to some erroneous conclusions and did not agree with many experimental observations. Recent theoretical results are from a variety of calculations based on modified intermediate neglect of differential overlap, *ab initio* Hartree Fock, molecular dynamic (MD) calculations. Calculations that include relaxation of the host crystal around a H impurity seem to lead to conclusions that are in agreement with the experimental results. Theory has also provided information regarding a variety of parameters that establish minimum energy locations and the migration path of various charge states in a Si lattice. These results are summarized below.

- The atomic H is stable at the bond center (BC) and tetrahedral (T) sites in several possible configurations. The most stable site for H in Si is the BC site, which has a high electron density, and the next stable is the T site of low electron density.
- Isolated interstitial H can exist in three charge states— H^+ , H^0 , or H^- . The preferred state depends on the position of the Fermi level. Experimentally, one finds that the preference of being in a particular charge state seems to depend on the resistivity type. In a p-type Si, the positive H ion can assume a relaxed BC site—lying between a substitutional dopant and the host Si atom, slightly off $\langle 111 \rangle$ axis. In n-type Si, the T site is preferred.
- The H^+ has a stable lowest energy at the BC site. A donor level, ~ 0.2 eV below the conduction band edge, is associated with this location.
- The H^- is stable at the T site. The location of the acceptor level associated with this site is not well defined. Some experimental measurements have identified two levels. One estimate is 0.06 eV below the conduction. The H^- has an activation energy for diffusion of at least 0.8 eV.
- It may be noted that both the donor and the acceptor levels appear in the upper half of the bandgap.
- A neutral H (H^0) is metastable. Its lowest-energy state has trigonal symmetry at a relaxed BC site, but it also exists at the T site. The energy difference between the two states is of the order of a few tenths of an eV—0.3 eV higher at the T site.

Hydrogen can form two kinds of dimers: an interstitial H_2 as molecules and an H^*_2 complex, which consists of two Si-H bonds replacing a single Si-Si bond. One H is near the BC site and the other is in an antibonding position, with the two H's on the same trigonal axis. This complex anneals out at about 200°C. Molecular H is generally seen in Si material grown in an H-containing ambient, exposed to H_2 gas at high temperatures or exposed to a H plasma. The importance of H_2 is in the fact that it can exist in “hidden” form because it is not optically active. However, during device processing, H_2 may dissociate, releasing atomic H that can diffuse and participate in passivation.

The structure of H in the Si lattice can be used to establish migration paths of H. The H^+ can jump from one BC site to another with an activation energy of 0.48 eV. This appears to be the favored diffusion path. Because the BC site is preferred in P-type Si, it is expected that diffusivity will be higher in P-type Si than in N-type Si.

Hydrogen Interactions with Impurities

Hydrogen interacts with many impurities, both dopants and nondopants, and deactivates them. Deactivation of shallow dopants, both p- and n-type, are well known. For example, H forms a complex (or

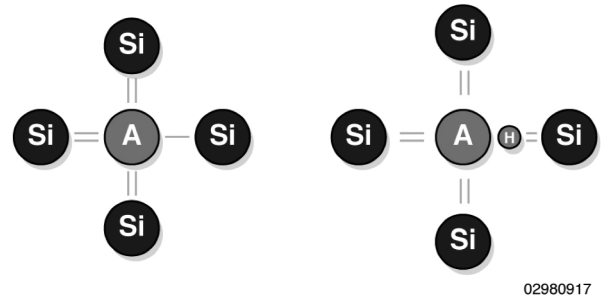


Fig. 3. Illustration of H bonding with an acceptor in Si.

a pair) with shallow acceptors such as B. This complex has a threefold coordinated B with H tying up the fourth Si bond in a near-BC position. Figure 3 illustrates the formation of such a complex; here, A is an acceptor ion. The pair has a dissociation energy of ~ 0.7 eV and readily dissociates at a temperature of $\sim 250^\circ\text{C}$. A similar complex is formed in which P is threefold coordinated with a lone pair along the trigonal axis, and H weakly binds to the fourth Si atom at the antibonding site. Formation of this complex is less efficient because it involves the slow-diffusing H at T sites, or the neutral species at BC sites. The {P, H} pair has a dissociation energy of 1.2 eV and breaks up around 200°C. Thus, H diffusing in a Si lattice can be trapped by the dopant if the temperature is less than the dissociation temperature.

Hydrogen also forms complexes with transition metal (TM) impurities. The TM-H complexes with Ti, Co, Ag, Pt, Pd, Ni, and Cu have been detected primarily by deep level transient spectroscopy (DLTS) analyses.^{28–30} In some cases, equilibrium structures for TM-H complexes have been calculated.³¹ Interestingly, the DLTS data do not verify that the complexes are electrically inactive. It appears that H only shifts the position of the TM energy levels within the gap, but no passivation (empty gap) occurs. Likewise, there is no experimental or theoretical information on the passivation of TM precipitates. These are important issues for fabrication of high-efficiency solar cells on low-cost Si substrates. These substrates contain TMs in soluble as well as precipitated forms, and it is necessary to either remove them by gettering or passivate them before they can yield high-efficiency solar cells.³²

Interactions of H with C and O can be very significant because these impurities are present in high concentrations in most Si devices, but there is very little pertinent information available for C. Recently, there has been a flurry of results on interactions between H and interstitial oxygen (O_i). It has been reported that the growth of O-related thermal donors in Czochralski silicon (CZ-Si) is greatly enhanced if the material is grown in an H_2 ambient. This mechanism appears to be caused by the tendency of O_i to attract isolated H and H_2 . On the other hand, in the temperature range of 300–450°C, H acts as a catalyst to enhance the diffusion of O. In oxygen-rich Si samples, three lines associated with H_2 are seen by Fourier transform infrared spec-

trospectroscopy (FTIR),³³ two of which are associated with H₂ trapped near interstitial oxygen (O_i). The binding energy of H₂ to O_i is 0.26 ± 0.02 eV, and the activation energy for diffusion of H₂ is 0.78 ± 0.05 eV. Isolated H₂ is seen³⁴ following anneals up to 350°C. This is of particular importance because H behaves differently in CZ than in float zone (FZ) Si.

Two models have emerged to explain enhancement of O diffusivity by H. In the first, H lowers the activation energy for O diffusion by tying up a Si dangling bond at the transition point. In the second, obtained from MD simulations, a covalent H-O pair forms, which transforms the stiff Si-O-Si bridged bond into a H-O-Si bond, with the {H, O} pair now able to rotate around the fixed Si atom, allowing it to visit the adjacent BC site. This problem is not completely understood.

Hydrogen Interactions with Native Defects

Hydrogen readily interacts with defects in Si primarily by passivating the dangling bonds. Because the Si-H bond strength is greater than that of a Si-Si bond, H can completely passivate the dangling bond site. It can also interact with weakly reconstructed bonds that are found at vacancies (V's) or clusters of V's. Hydrogen rarely forms perfect Si-H bonds within the crystal, because the Si bonds at the V and at clusters of V's undergo some degree of reconstruction. On the other hand, there is some evidence that H can even activate some aggregates of vacancies. For example, the hexavacancy complex (V₆), by itself, is almost totally inactive, but it becomes electrically active upon trapping H.³⁵

Self-interstitial (I) and I aggregates also trap H, but their thermal stability is low (maybe 200°C or less). Only one {I, H, H} complex has been identified by FTIR and ab-initio theory.³⁶ Its vibrational modes are at 1987 and 1989 cm⁻¹, below those of {V_n, H} complexes. The binding energies are small, ranging from

2.6 eV for {I, H, H}, down to 1.5 eV for {I, H}, and just a few tenths of an eV for {I, H, H, H}. Contrary to earlier theoretical predictions,³⁷ it appears that this complex is not passivated by H and it requires at least four H atoms to passivate a single I. The capability of H to passivate point defects and point defect clusters is exploited in a-Si to improve its photoconductivity and make it suitable for solar cell applications.

Hydrogen can passivate extended defects such as dislocations, stacking faults, and grain boundaries, primarily by saturating their dangling bonds. This would be the case in "clean" defects in high-quality material such as poly-Si used for TFT applications. Here, H is known to improve the lateral carrier transport across grain boundaries. However, in most cases, extended defects have segregation of impurities or are even decorated with the impurity precipitates. There is some question whether H can passivate decorated extended defects. In the case of clean defects, H can rapidly diffuse along the defects and segregate at sites of local stress. It is believed that, like TM impurities, H can segregate at kink sites of dislocation networks or grain boundaries. Figure 4 shows transmission electron microscopy (TEM) photographs of hydrogenated multicrystalline Si showing segregation of H in the form of "bubbles" at dislocations and at a grain boundary. Here, the grain boundary is perpendicular to the surface. It is clear that the size of the defect caused by H segregation is larger near the surface.

Extended Defects Caused by H

In addition to the direct interaction with Si defects, H can form its own defects. In many cases, the formation of H defects is a combination of the damage produced by the hydrogenation process and the interaction of the damage with H. Figure 5 is a cross-sectional TEM photograph of the defects generated near the surface of a Si wafer by a 1.5 keV

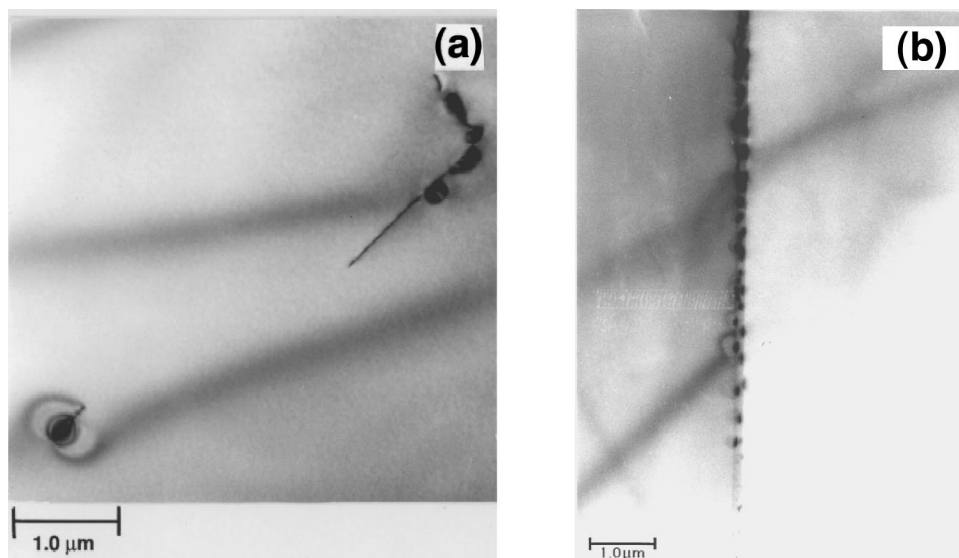


Fig. 4. XTEM photos of hydrogenated Si samples, showing segregation of H (a) at the dislocations and (b) along a grain boundary.



Fig. 5. XTEM photo showing defects generated near the surface by a 15 KeV H implantation.

implant at 250°C. These defects are primarily dislocation loops with a large concentration of H associated with them. When large concentrations of H are present and the sample is at an elevated temperature, H can lead to segregation into “bubbles” and formation of platelets.

Platelets are disclike microdefects that lie along {111} planes and are elongated along [110] directions. Cross-sectional TEM pictures of platelets are shown in Fig. 6. Figure 6(a) shows a series of platelets, identified by arrows, generated at the surface of a hydrogenated Si sample. Figure 6b is a higher-magnification picture showing one tilted platelet. It is seen that such a defect has a corelike structure. The core of the platelet is believed to consist of vacancy clusters that may have some trapped molecular H.³⁸ The platelets are excellent sinks for interstitial impurities and have been shown to be efficient for gettering transition metals.³⁹ Under the same conditions of implantation, the samples having a lower concentration of oxygen exhibit deeper penetration of the defect.

METHODS OF HYDROGENATION

Hydrogen can readily diffuse into Si when exposed to atomic H. Thus, H can be introduced into Si

by a variety of processes that can generate atomic H. Such methods can be categorized as (1) electrochemical systems, (2) plasma-based systems, (3) ion implantation, and (4) molecular ambient systems.

Electrochemical systems can provide a reasonably high density of hydrogenic species at the surface of a Si wafer. Simple treatments such as dipping a wafer in boiling water, dipping in dilute HF, and etching in an HF:HNO₃ solution can provide copious amounts of H in Si. A technologically important issue regarding the high diffusivity of H is that H can be incorporated in Si at room temperature by such processes as cleaning and etching in solutions that contain HF. For example, in a standard process used extensively in wafer cleaning and oxide stripping, a dilute HF dip can lead to diffusion of H several microns below the surface. Although significant amounts of H can be introduced near the surface by these methods, this is basically a low-temperature process. Consequently, this process is limited by diffusivity of H and trapping mechanisms. This method could be well suited for dopant deactivation near the surface (e.g., to form a junction).

A plasma process can offer a high-density source of atomic H, and the equipment is commercially available. Standard dc or rf plasma may have energy of several hundred volts, which produces some surface damage. Such surface damage actually has an advantage in that it increases the concentration of trapped H near the surface (allowing more H to diffuse into the material). However, the presence of surface damage leads to a high surface recombination. To reduce the energy of the ion impinging the device or a wafer, the ion may be transported away from the direct plasma, and, in some cases, the ion can be slowed to minimize the damage.

To lower the damage further, the electron-cyclotron resonance technique is useful. It allows operation under lower pressure, typically 10⁻⁴ torr, and ion energy of a few tens of electron volt (eV).

A higher-throughput approach that has been used in solar cell processing is the Kaufman ion source using an unpolarized beam. Typical ion implanta-

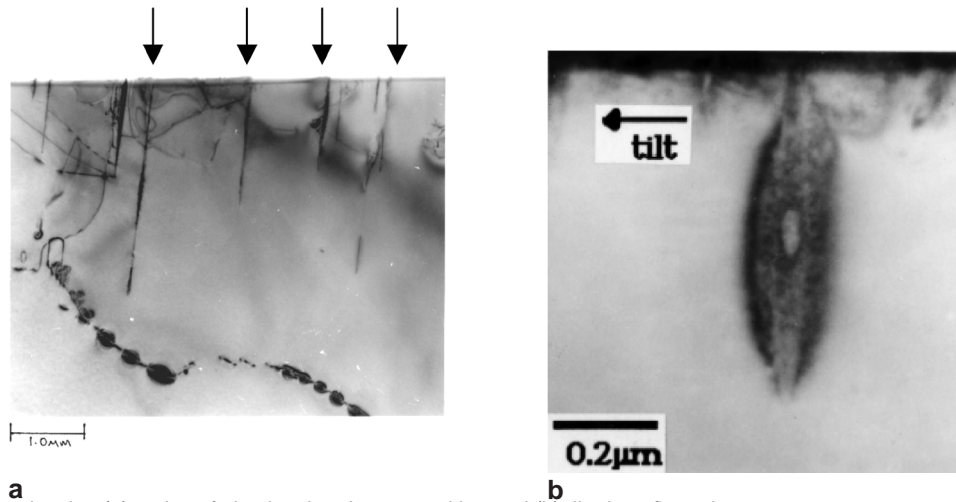


Fig. 6. XTEM photos showing (a) series of platelets in edge-on position and (b) tilted configuration.

tion uses beam energy <1 keV, and a current density of about a 0.5 mA/cm², at a temperature of about 250–300°C. Standard ion implantation with energy exceeding a few hundred eV can be used, but is not suitable for high throughput processes.

An interesting approach for H diffusion is to provide an H-rich surface film that can release H on subsequent processing. This method is used in Si solar cell manufacturing. A plasma-enhanced chemical vapor deposition (CVD) (PECVD) process is used to deposit a layer of Si₃N₄ that is rich in H. Use of a plasma process is expected to provide initial indiffusion, as well as a source of H. This method has a high potential in solar cell passivation.

The simplest method of introducing H into Si is thermal anneal in forming gas, which has been successful for MOS devices. This method of H processing is used in commercial fabrication of all MOS devices as postmetal annealing (PMA) in forming gas. This process was conceived long before details of H diffusion were known. The PMA was found to remove both characteristic interface states and the interfacial paramagnetic defect center in the MOS structure.^{40,41} A typical 10 min, 450°C anneal in 10% H-nitrogen forming gas reduces the midgap D_{it} to an acceptable 10¹⁰ cm⁻² eV⁻¹ range. The mechanism can be explained in terms of diffusion of atomic H to the interface to deactivate the interface trap. It is believed that molecular H₂ must dissociate before such diffusion is possible.

One of the two mechanisms may be responsible for such dissociation. One possibility is that the dissociation of H₂ occurs because of the presence of a metal located in the vicinity of a Si device. This is a likely case for MOS devices and is in agreement with the observation that the passivation does not occur in the absence of metal. The other possible mechanism is that H diffusion can occur in a Si wafer that has surface damage. It has been proposed that, here, the dissociation of H₂ occurs by the vacancies associated with the surface damage.^{42,43} Theoretical studies have shown that an H₂ molecule can be spontaneously dissociated by a vacancy. Although this mechanism leads to an important pro-

duction process for hydrogenation, especially for solar cells, the presence of damage at the surface is not desirable. Surface damage can be introduced by a variety of processes including mechanical abrasion, plasma processing, and ion implantation. These processes are used in the formation of N/P junctions and Si₃N₄ layer deposition (e.g., depositing an antireflection coating on solar cells).

For MOS device applications, H must only reach the surface of a Si wafer. Here, H must diffuse through a thin layer of an oxide to a SiO₂/Si interface. In the case of a-Si solar cells, the hydrogenation occurs simultaneously during the deposition of a-Si. However, for most other device applications, H is introduced after device processing. Some devices such as crystalline (or multicrystalline) Si solar cells or polycrystalline layers for TFT applications require deep diffusion of H. Because solar cells are minority-carrier devices, they require that the entire thickness of the cell be passivated. Typically, these processes are not high-throughput processes. The primary objective of the hydrogenation process is to allow H to diffuse into the device or substrate and to find its way to passivate impurities and defects. In general, there appears to be little control on how to optimize a specific favorable interaction. The only way to control the interaction appears to be the temperature of hydrogenation and the cooling rate.

HYDROGEN DIFFUSION IN SILICON

Diffusivity of H is an important parameter, not only for process design but also for understanding diffusion mechanisms. The experimental data on the diffusivity and solubility of H in Si were obtained by van Wieringen and Warmoltz.²⁶ They performed experiments to measure permeation of H, He, and Ne, through thin-walled Si cylinders from 1090°C to 1200°C. They expressed the diffusivity of H (D_H) as

$$D_H = 9.67 \times 10^{-3} e^{-\frac{1}{kT}(0.48eV)} \text{ (cm}^2/\text{sec)}$$

This diffusivity is expected to remain valid down to low temperatures. Figure 7 shows a solid line representing the results of diffusivity as a function of

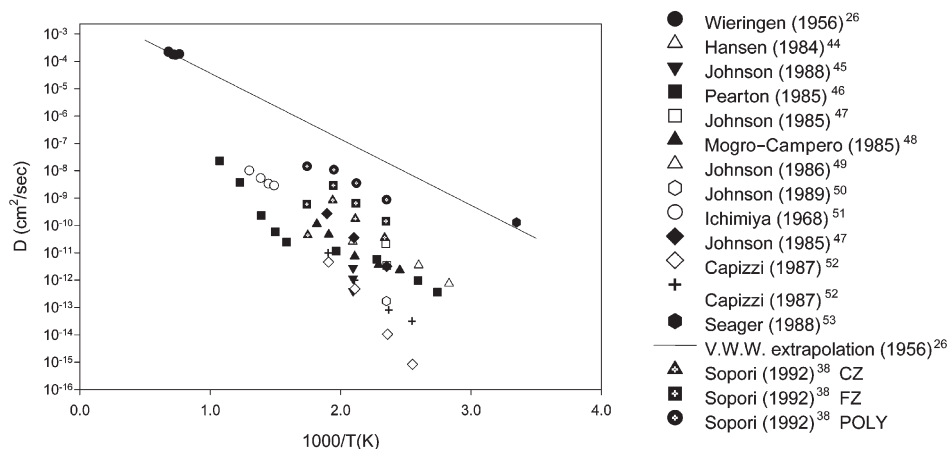


Fig. 7. Diffusivity of H reported by various researchers.

temperature. The diffusivity at room temperature is $8.3 \times 10^{-11} \text{ cm}^2/\text{s}$. In later experiments, diffusivity measurements were performed on wafers using H, deuterium, and tritium. The various data are compiled and are shown in Fig. 7. It is apparent in Fig. 7 that there is a large variation in the diffusivity of H. This apparent variation in D_H may indicate that more than one mechanism is involved in the diffusion of H, or the diffusion characteristics are strongly influenced by the material quality.

Recent studies have shown that, indeed, H diffusion is strongly influenced by the impurities and defects in the device or wafer. As mentioned in the previous section, H can form complexes with impurities and defects that are stable at low temperatures. This mechanism can result in trapping of H. For example, if H diffusion is done at temperatures of less than about 200°C , the H can be trapped as H-B pairs, leading to a significantly lower “effective diffusivity.” The trapping effects are manifested as kinks in the diffusion profile that also result in deviations from an erfc profile. Later in this section, we will present a coherent model that includes the trapping effects to show the influence of traps on H diffusion.

The diffusivity measured at high temperature in Ref. 26 was thought to correspond to that of H_2 molecules. But, it is now known that this diffusivity corresponds to a fast-diffusing H at a the BC site. The molecule diffuses much more slowly, with $E_a = 0.78 \text{ eV}$, while H at T sites diffuses even slower. The only species that can diffuse faster than BC is the metastable state that corresponds to H^0 at T sites.¹⁷

It is instructive to examine the effect of trapping on the diffusion behavior of H. Recently, some theoretical analyses have been done that include the effect of uniform trap density within the bulk of a material. Although inclusion of bulk traps results in a better fit to measured diffusion profiles, it does not predict the high concentrations of H that are observed near the surface of a hydrogenated wafer, nor does it explain the dependence of diffusion profiles on hydrogenation processes. Here, we briefly describe a model that includes the influence of the grown-in traps in the material and those introduced during processing.⁵⁴ As expected, the nature and distribution of process-induced traps is a strong function of the hydrogenation process itself and is, in general, time dependent. Here, we will use this model to primarily illustrate the effects of hydrogenation, including various trapping processes, on the profile of H.

Mathematically, we can include trapping in the diffusion equations and write it as

$$\frac{\partial[\text{H}_{\text{untrapped}}]}{\partial t} = D_H \frac{\partial^2[\text{H}_{\text{untrapped}}]}{\partial x^2} - \frac{\partial[\text{H}_{\text{trapped}}]}{\partial t}$$

$$\frac{\partial[\text{H}_{\text{trapped}}]}{\partial t} = k[\text{H}_{\text{untrapped}}][\text{T}_{\text{unoccupied}}] - k'[\text{H}_{\text{trapped}}]$$

We can impose the following conditions describing the interaction of H and traps:

$$[\text{H}_{\text{tot}}] = [\text{H}_{\text{untrapped}}] + [\text{H}_{\text{trapped}}]$$

$$[\text{T}_{\text{unoccupied}}] + [\text{H}_{\text{trapped}}] = [\text{T}_{\text{tot}}]$$

where

$[\text{H}_{\text{untrapped}}]$ = concentration of mobile H

$[\text{H}_{\text{trapped}}]$ = concentration of trapped H

$[\text{H}_{\text{tot}}]$ = total H concentration

$[\text{T}_{\text{tot}}]$ = total trap density

Here, k' is the dissociation frequency and k is the association rate. In our calculations, we will assume a reasonable value of dissociation frequency (see the “Results and Discussion” section). The association rate can be expressed in terms of the effective capture cross section (radius), R_c , as $k = 4\pi R_c D_H$.

These equations need to be solved under boundary conditions (B.C.s) imposed by the hydrogenation process. The B.C.s used for the simulation are depicted as follows:

$$[\text{H}_{\text{untrapped}}]_{x=0} = C_s \text{ for a constant surface concentration, } C_s, \text{ of mobile H in plasma process}$$

$$-D_H \left. \frac{\partial[\text{H}_{\text{untrapped}}]}{\partial x} \right|_{x=0} = J_s \text{ for a constant flux of mobile H for implantation process}$$

Usually, the sample is thicker than the penetration depth of H. The following B.C. at $x = x_c$ was adopted, where x_c is a cutoff depth that is greater than the penetration depth of the H diffusion.

$$\left. \frac{\partial[\text{H}_{\text{untrapped}}]}{\partial x} \right|_{x=x_c} = 0$$

We will assume traps to be immobile, and apply this model to illustrate the influence of various trapping mechanisms on the diffusion profile. To demonstrate the effects of process-induced traps, we use the experimental data from Ref. 55 of a B-doped ($1.3 \times 10^{18} \text{ cm}^{-3}$) sample for plasma processed at 200°C for three different time durations (5 min., 10 min., and 15 min.). Here, a uniform bulk trap level that coincides with the doping level is assumed. For plasma processing, the form of process-induced trap distribution is expected to be exponential with a time-independent surface concentration. The total trap density has the following time dependence:

$$[\text{T}_{\text{tot}}] = T_0 \exp\left[-\frac{x}{a+bt}\right] + T_b$$

where the first time-dependent term is due to process damage and T_b is a constant bulk trap level. The best fits are obtained with $T_0 = 10^{21} \text{ cm}^{-3}$, $a = 0.1 \mu\text{m}$, $b = 0.108 \mu\text{m}$, and $T_b = 1.3 \times 10^{18} \text{ cm}^{-3}$. These results are shown in Fig. 8. The solid lines show the fitted data. The best fits are obtained if we assume the dissociation frequency $k' = 0.2$. It should be noted that the same set of parameters

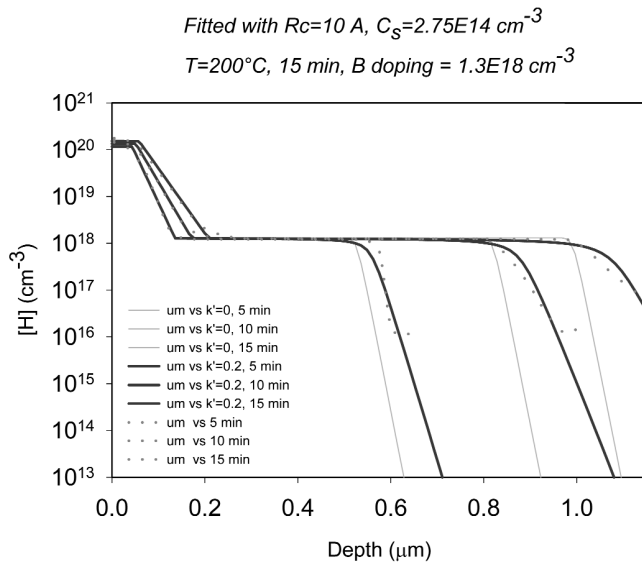


Fig. 8. Experimental data of Ref. 55 (dotted lines) and fitted results.

gives an excellent fit for experimental profiles for different times. For comparison, we have also simulated profiles for zero dissociation rate; these are shown in thin, densely dotted lines.

These results clearly show that tapping can retard the diffusion of H, and it only requires small values of C_s to match the experimental data. We can also look upon traps as “storage sites” for H. We have used this concept to explain H passivation of solar cells by the plasma CVD nitridation process.⁵⁶

It is interesting to point out that one of the proposed H diffusion mechanisms involves interaction of H with vacancies is a [V, H] pair. This mechanism was invoked to reconcile the fact that the measured D_H depends on the vacancy concentration in the material.⁵⁷ Figure 9 shows the measured D_H values for five substrates grown by different techniques.

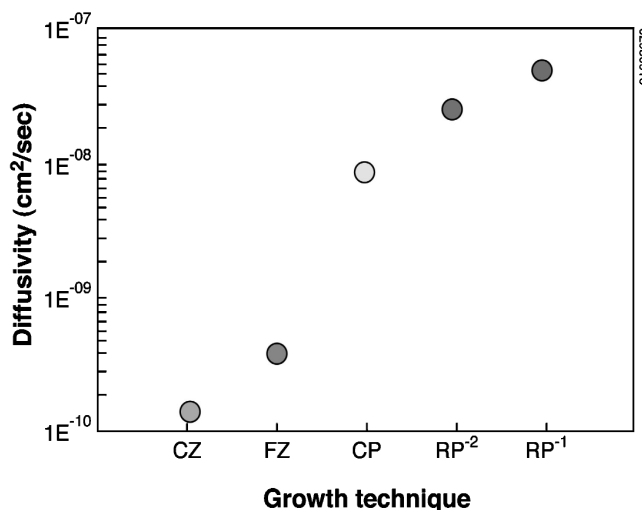


Fig. 9. A plot showing measured diffusivity of various types of substrates. CZ—Czochralski, FZ—float zone, CP—cast poly-Si, RP²—ribbon Si (multicrystalline) grown by edge defined film fed growth, and RP¹—ribbon grown by ribbon-to-ribbon growth by laser recrystallization.

Positron annihilation spectroscopy of various types of Si substrates showed that the vacancy-related defect density was higher for the substrates that showed higher D_H . These results are in agreement with the [H, V] diffusion model. They also suggest that a process that injects vacancies during hydrogenation can exhibit enhanced diffusion.

The [H, V] mechanism can explain the experimentally observed dependence of D_H on the oxygen concentration. Figure 10 shows the diffusion profiles of H in two samples from an ingot that differs only in the oxygen concentration. The measured diffusivities are $1.5 \times 10^{-8} \text{ cm}^2/\text{s}$ and $2.4 \times 10^{-9} \text{ cm}^2/\text{s}$ for the samples containing oxygen concentrations of 8.4 ppma and 12.2 ppma, respectively. This can be attributed to a reduction in vacancy concentration accompanying a higher O concentration. It is also interesting to note that the effective solubility of both samples is the same.

Thus, vacancies can play an important role in hydrogenation. Figure 11 shows an integrated model that we have developed to explain H passivation mechanisms in Si solar cells, for plasma as well as for forming gas hydrogenation. It shows hydrogenation of a typical solar cell having a front N/P junction and a rear metal contact. The junction is accompanied by surface damage because of a high concentration (and precipitation) of P. Here, the atomic H, having enough energy to overcome the surface barrier, enters the wafer. The surface region has a high solubility of H caused by the damage. The damaged layer can dissociate H_2 and result in the formation of an [H, V] pair. Thus, H can diffuse as atomic H or via a vacancy mechanism.⁵⁷ An [H, V] mechanism would be favored in vacancy-rich substrates such as cast or ribbon Si.

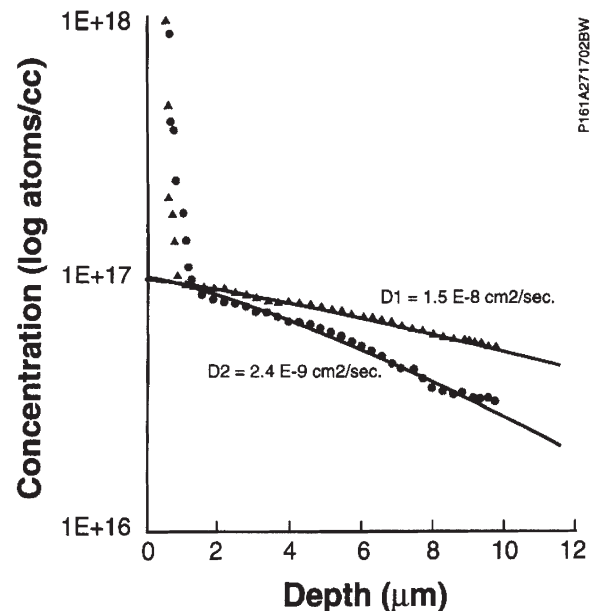


Fig. 10. SIMS profiles of H diffusion in two wafers in the same ingot that vary in O concentration. Hydrogen was implanted at 1.5 KeV, at 250°C.

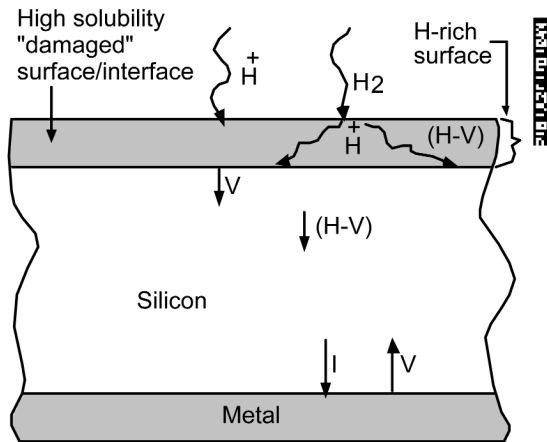


Fig. 11. A sketch illustrating various mechanisms that take place during hydrogenation of a Si device.

HYDROGEN AND DEUTERIUM IN SILICON DEVICES

Because H can readily passivate interfaces, defects, and impurities in the semiconductor, it may be used to improve many devices whose performance is limited by minority-carrier recombination resulting from the deep levels induced by impurities and defects. To date, H passivation is extensively used in the fabrication of MOS devices, a-Si and c-Si solar cells, and poly TFTs.

As mentioned in previous sections, H treatment (e.g., a PMA step) is routinely used in fabricating MOS transistors to improve the characteristics of the Si/SiO₂ interface by passivating the defects (traps) located in the vicinity of the interface. Each of the traps may possess one or more energy levels within the bandgap. These energy levels can interact with Si by capturing or emitting carriers from the conduction and valence bands. An increase in interface trap density can cause shift of threshold voltage (V_T) and alter drain current (I_D) vs. gate voltage (V_G) characteristics of affected devices. This damage to individual CMOS transistors and inverters can result in increased current supply (due to increased leakage currents or through transistors turning on what should be off), logic failures, latchup effects, or changes in the circuit timing. As the individual transistors making up a complicated CMOS integrated circuit are degraded, the characteristics of the overall circuit will become increasingly unpredictable.

The PMA step was found to greatly diminish both the characteristic states and the defect centers at the SiO₂/Si interface. It is believed that a catalytic reduction of H₂ results in a release of atomic H at temperatures of 400–500°C.⁴ The atomic H subsequently diffuses across the oxide to the interfacial trap sites, where it passivates them by removing the energy states from the bandgap. Studies on the catalytic activity of Pd have clearly shown that this reaction takes place in the presence of gate metals.⁵⁸ However, sometimes the passivation is also seen when the gate metal is absent.⁵⁹ This suggests that

the possibility of reactions in the dielectric oxide or even at the Si/SiO₂ interface cannot be ruled out.

The properties of the SiO₂/Si interface are also important for high-efficiency Si solar cells. Most Si solar cells have a thermal surface oxide to reduce their surface recombination velocity. Again, a forming gas anneal may be used to accomplish such a reduction in the surface recombination, in a manner similar to that of a MOS device. However, because solar cells may also require passivation for bulk defects and impurities, other methods of hydrogenation may be used that can produce bulk and surface passivation simultaneously (see the next paragraph). It is, however, found that such an oxide exhibits degradation upon exposure to UV. The mechanism of degradation is believed to be similar to that of the hot-electron effect.

Hydrogen is a major constituent in a-Si solar cells. These devices contain a large fraction of H, as much as 5–10%, which is introduced by H dilution during a-Si deposition. Hydrogen passivation is used in nearly all commercial Si solar cells fabricated on low-cost, multicrystalline substrates. Hydrogenation can lead to a significant increase in the cell efficiency by as much as 20%. In contrast with MOS devices that require interface passivation only, the hydrogenation in solar cells requires passivation within the entire thickness of the device and the surface. Thus, H diffusion in PV materials is an especially important topic. Such a passivation process usually leads to a reduction in the dark current of the cell and an increase in the photocurrent. Figure 12 shows I-V characteristics of an N/P-type cell before and after passivation. Currently, the most common method for H passivation is a two-step process consisting of (1) deposition of a Si₃N₄ by a low-temperature PECVD process and (2) a rapid thermal anneal (RTA) that diffuses H deep into the bulk of the device. The major effect of passivation is observed only after the RTA process. The details of the H diffusion

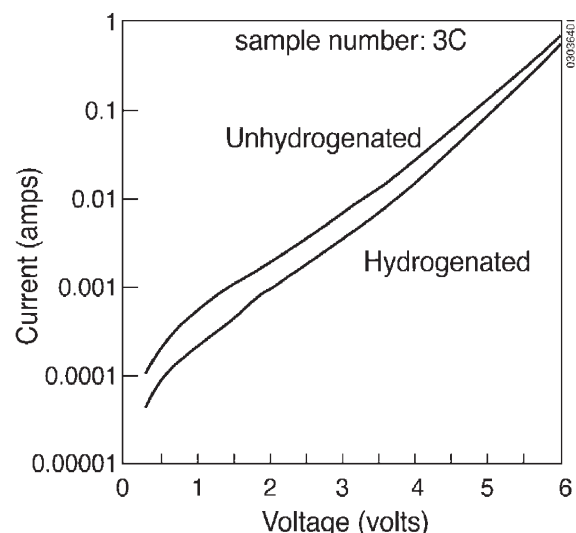


Fig. 12. Dark I-V characteristics of N/P Si solar cell before and after passivation.

during these process steps have not been established. A possible two-step diffusion mechanism is proposed in Ref. 56. It is believed that an accumulation of H occurs at the traps near the surface of the solar cell during the Si_3N_4 deposition. The trapped H dissociates during the following RTP anneal and diffuses through the entire device. Figure 13 shows the internal spectral response (quantum efficiency) of a solar cell before and after passivation by a PECVD nitride. It is seen that there is an increase in the red response indicative of an improvement in the minority-carrier diffusion length. There is, however, a decrease in the short quantum efficiency at short wavelengths; it is believed to be due to the fact that the Si_3N_4 is not stoichiometric but is rich in Si, absorbing light at short wavelengths in the deposited film.

Hydrogen also has potential applications in poly-Si TFTs. Here, the objective of H is to passivate dangling bonds associated with grain boundaries. This results in an increase in the lateral conductance of the grain boundaries. However, the extent of such diffusion should be justified. If excessive H is incorporated, H may induce its own defects in the lattice or along the grain boundary. We have observed that excessive hydrogenation can result in formation of defects caused by segregation of H from the bulk to the grain boundary, as shown in Fig. 4b.

The time-dependent degradation of MOS transistor performance resulting from the hot-electron effect has been a challenge for many researchers. One explanation is that the degradation involves the de-passivation of bonded H at the interface by positively charged $\text{H}^{60,61}$. The idea of using deuterium instead of H to passivate a MOS structure was, in part, inspired by experiments in which a scanning tunneling microscope STM was used to stimulate the desorption of H from $\text{Si}(100)2 \times 1:\text{H}$ surfaces under ultrahigh vacuum conditions.⁶² Experimentally, substitution of H by deuterium in the PMA of MOS devices resulted in improvement in the device operational lifetime.⁶³ The devices were n-channel MOS transistor structures fabricated using the Bell Laboratories (Murray Hills, NJ) $0.5 \mu\text{m}$ 3.3 V CMOS

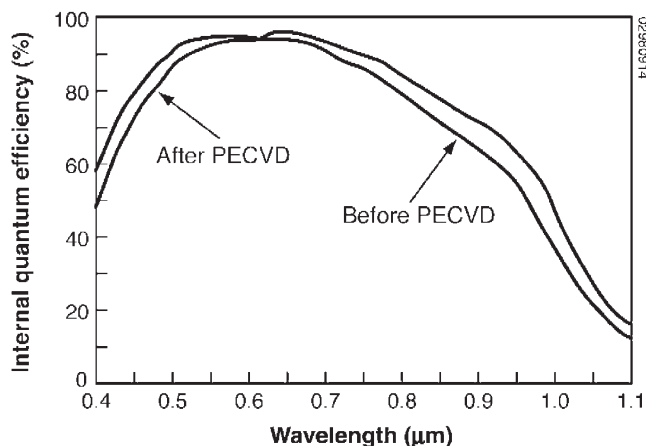


Fig. 13. Internal quantum efficiency of a Si solar cell before and after H passivation by PECVD nitride.

technology with a slight modification of process conditions to enhance the hot electrons. A degradation of 20% in g_m was used as a lifetime criterion, and lifetimes were found to be 10–50 times longer than those sintered in H. By considering a shift of 200 mV in threshold voltage as the degradation criterion, a factor of 10 improvement of lifetime was seen. Subsequent studies^{64,65} showed evidence of improvements in the device performance of different structures, such as transistors of $0.2 \mu\text{m}$ channel length, standard $0.35 \mu\text{m}$ devices from major companies, devices with SiO_2 or Si_3N_4 sidewall spacer, and even for those after SiN cap process. A recent study,⁶⁵ in which a finished MOS device was subjected to high pressure (6 atm), 100%- D_2 anneal at 450°C for 3 h, exhibited a significant ($90\times$) improvement in lifetime. Furthermore, a similarity in degradation behavior (i.e., dependence on interface states) of g_m and V_T in H_2 - and D_2 -annealed devices supported the hypothesis that the hot-electron stressing creates interface states.

Several models were proposed to explain higher stability of deuterium. In one case, it was attributed to larger zero-point energy of Si-H oscillations as compared to Si-D, and the effect of the possibility of excited Si-H or Si-D oscillation for different masses. Another explanation was that the hot electrons in the channel excite the electron of the Si-H(D) bond into an antibonding state. This change in configuration results in a force that accelerates H(D) away from the surface and leads to dissociation. Deuterium, because it is twice as heavy, does not accelerate as rapidly and the electron returns to the bonding state before dissociation occurs. Some observations have been made⁶⁶ that the vibrational mode frequencies of the Si-H and Si-D modes are different and that the latter has a bending mode close to a bulk phonon mode of a Si lattice (460 and 463 cm^{-1} , respectively). Coupling of these modes may provide an energy relaxation pathway, making dissociation of the Si-D bond more difficult than for Si-H. However, the exact mechanism of this isotopic interfacial “hardening” remains uncertain.

Similar to the degradation problem with MOS devices, a-Si solar cells exhibit such a behavior caused by illumination (Staebler–Wronski effect). In solar cell applications, single-junction p-i-n amorphous Si solar cells were attempted in Refs. 67 and 68. Deuterium was used to replace the H in the intrinsic layer of the cell. Light exposure at 50°C under one-sun illumination was carried out. The measurement of cell parameters and bonding investigated using infrared secondary ion mass spectroscopy (SIMS) showed higher open-circuit voltage (V_{oc}) and lower short-circuit current density (J_{sc}) for the deuterated cell as compared to the hydrogenated cell. Quantum efficiency vs. wavelength data revealed a similar short wavelength ($\lambda < 500 \text{ nm}$) response, whereas the long wavelength ($\lambda > 500 \text{ nm}$) response accounts for the 2 mA/cm^2 difference in photocurrent, indicating a wider bandgap in the deuterated cell. The

deuterated cells show a higher stabilized fill factor (FF) than the hydrogenated cells. The best FF of 0.655 was obtained for a deuterated cell with an i-layer thickness of 310 nm. The D content in the deuterated material is higher than the H content in the hydrogenated material. The light-induced photoconductivity degradation in an intrinsic hydrogenated and deuterated a-Si alloy was monitored under AM1 illumination for up to 600 h. It was found that both the dark conductivity and photoconductivity had increased by a factor of 6 or 7. A similar mechanism was proposed to explain this phenomenon and was compared to the case of SiO₂/Si. It was attributed to the highly efficient coupling between the localized Si-D wagging mode ($\sim 510 \text{ cm}^{-1}$) and the extended Si-Si lattice vibration mode (495 cm^{-1}).

There have been some explanations about the advantage of deuterium over H, but questions still remain for further investigation. Some studies on MOS structures in which photoinjection was used to introduce electrons into the oxide demonstrated no significant difference between D- and H-passivated interfaces.⁶⁹ These results may suggest that physical differences exist between the hot-electron and light-irradiation degradation mechanisms. References 67 and 69 showed that a MOS device, fabricated by standard technology but with PMA performed in D₂, had comparable concentrations of H and D. This shows that a H containing ambient is quite prevalent in the CMOS back-end process, and there is an abundance of H in interlevel dielectrics. The effectiveness of deuterium, even with abundant H content coexisting near the interface, remains a question.

SUMMARY AND CONCLUSIONS

We have presented a brief review of some technologically important aspects of H in Si. Examples of fundamental aspects of H interactions with the perfect Si lattice and impurities and defects were discussed. The primary effect of H is to passivate the dangling bonds in Si. This propensity for interaction with the dangling bonds makes H very reactive to defects and impurities. Hydrogen is used in the fabrication of MOS devices and solar cells because it can passivate interfaces and extended defects. The improvements in the device performance are primarily through reduced recombination of carriers at the defect and impurity sites. Hydrogen does not seem to passivate all types of defects and impurities. In fact, it is believed that complexes of interstitials and vacancies are made electrically more active by H. Likewise, there is no evidence that H passivates precipitated impurities.

Hydrogen introduces its own defects that can be detrimental to the devices. Some observations of H segregation along the dislocations and grain boundaries (bubbles) and near the surface (platelets) were presented. Trapping at defect and impurity sites was used to explain the observed high solubility (and low diffusivity) of H in Si, which should be oth-

erwise extremely low (and high) as derived from the high-temperature experiments. A coherent way of understanding diffusion in Si is to consider migration from one interstitial site to another, as well as hopping among defect/impurity sites caused by trapping and detrapping. We presented examples of theoretical modeling of H diffusion through process-induced and bulk trapping. For example, in boron-doped samples hydrogenated at 200°C, theory yielded excellent fits with the experimental profiles. An important result was that the process-induced traps near the surface can have a strong influence on the H diffusion. Trapping is also important as a means of "storing" H in Si. This concept is used in solar cell passivation; H is "stored" near the device surface by depositing a PECVD Si nitride layer and then diffused by an RTP anneal. The traps, themselves, may be annealed out and have little influence on the device. Finally, recent research activities on improved stability by substitution of H by deuterium were reviewed.

Various hydrogenation methods were categorized and reviewed with respect to their use for device processing. These methods include electrochemical methods, plasma and ion beam techniques, PECVD, and forming gas anneal. Hydrogenation has already found a wide range of applications in junction formation, solar cell passivation, and MOS transistor interfacial state passivation. Newer applications will be realized as we learn more about H in Si.

ACKNOWLEDGEMENTS

This work was supported by the U.S. Department of Energy under Contract No. DE-AC36-00G010337 and by the DOE Center of Excellence for Advanced Materials Processing. The authors are very grateful to Kim Jones and Robert Reedy for many valuable comments and for performing the TEM and SIMS analyses, respectively.

REFERENCES

1. J.I. Pankove, M.A. Lampert, and M.L. Tarnag, *Appl. Phys. Lett.* 32, 439 (1978).
2. J.I. Pankove and M.L. Tarnag, *Appl. Phys. Lett.* 34, 156 (1979).
3. N.M. Johnson, *Hydrogen in Semiconductors, Semiconductors and Semimetals*, ed. J.I. Pankove and N.M. Johnson (New York: Academic Press, Inc., 1991), vol. 34, pp. 37–38.
4. E.H. Nicollian and J.R. Brews, *MOS (Metal Oxide Semiconductor) Physics and Technology* (New York: John Wiley, 1982), p. 781.
5. M.H. Brodsky and R.S. Title, *Phys. Rev. Lett.* 23, 581 (1969).
6. M.H. Brodsky and R.S. Title, *AIP Conf. Proc.* 31, 97 (1976).
7. A. Matsuda and K. Tanaka, *J. Appl. Phys.* 60, 2351 (1986).
8. D.L. Staebler and C.R. Wronski, *Appl. Phys. Lett.* 31, 292 (1977).
9. D.L. Staebler and C.R. Wronski, *J. Appl. Phys.* 51, 3262 (1980).
10. C.H. Seager and D.S. Ginley, *Appl. Phys. Lett.* 34, 337 (1979).
11. N.H. Nickel, N.M. Johnson, and W.B. Jackson, *Appl. Phys. Lett.* 62, 3285 (1993).
12. B.M. Abdurakhmanov and R.R. Bilyalov, *Renewable Energy* 6, 303 (1995).

13. E. Katz, M. Koltun, and L. Polyak, *Diffusion and Defect Data Pt. B, Solid State Phenomena*, p. 479 (1996).
14. J.D. Bernstein, S. Qin, C. Chan, and T.J King, *IEEE Trans. Electron. Dev.* 43, 1876 (1996).
15. C.M. Park, J.H. Jeon, J.S. Yoo, and M.-K. Han, *Mater. Res. Soc. Symp. Proc.* 471, 167 (1997).
16. C.T. Sah, J.Y.C. Sun, and J.J.T. Tzou, *Appl. Phys. Lett.* 43, 204 (1983).
17. C.T. Sah, J.Y.C. Sun, and J.J.T. Tzou, *J. Appl. Phys.* 55, 1525 (1984).
18. A. Endrös, *Phys. Rev. Lett.* 63, 70 (1989).
19. D. Tripathi, P.C. Srivastava, and S. Chandra, *Phys. Rev. B* 39, 13420 (1989).
20. S.J. Pearton and A.J. Tavendale, *J. Phys. C. Solid State Phys.* 17, 6701 (1984).
21. R. Singh, S.J. Fonash, and A. Rohatgi, *Appl. Phys. Lett.* 49, 800 (1986).
22. S.J. Pearton and A.J. Tavendale, *J. Appl. Phys.* 54, 1375 (1983).
23. S.J. Pearton and A.J. Tavendale, *Phys. Rev. B* 26, 7105 (1982a).
24. R.C. Newman, J.H. Tucker, A.R. Brown, and S.A. McQuaid, *J. Appl. Phys.* 70, 3061 (1991).
25. R.B. Capaz, L.V.C. Assali, L.C. Kimerling, K. Cho, and J.D. Joannopoulos, *Phys. Rev. B* 59, 4898 (1999).
26. Wieringen and N. Warmoltz, *Physica* 22, 849 (1956).
27. J.W. Corbett, D. Peak, S. Pearton, and A.G. Sganga, *Hydrogen in Disordered and Amorphous Silicon*, NATO ASI Series B, Physics, ed. Gust Bambakidis and R.C. Bowman, Jr. (New York: Plenum Press, 1986), vol. 136, pp. 61–79.
28. M. Stavola, *7th Workshop on the Role of Impurities and Defects in Silicon Device Processing*, Vail, CO, NREL/CP-520-23386 (1997), NREL, Golden, CO, p. 63.
29. J. Weber, *Mat. Res. Soc. Sym. Proc.* 513, 345 (1998).
30. J.U. Sachse, E.Ö. Sveinbjörnsson, N. Yarykin, and J. Weber, *Mater. Sci. Eng. B* 58, 134 (1999).
31. R. Jones, S. Öberg, J. Goss, P.R. Briddon, and A. Resende, *Phys. Rev. Lett.* 75, 2734 (1995); A. Resende, R. Jones, S. Öberg, and P. R. Briddon, *Phys. Rev. Lett.* 82, 2111 (1999).
32. B.L. Sopori, *Proc. 10th Int. Workshop on the Physics of Semiconductor Devices* (Delhi, Allied Publishers, Ltd., 2000), pp. 1214–1226.
33. R.E. Pritchard, M.J. Ashwin, J.H. Tucker, R.C. Newman, E.C. Lightowers, M.J. Binns, S.A. MacQuaid, and R. Falster, *Phys. Rev. B* 56, 13118 (1997); R.C. Newman, R.E. Pritchard, J.H. Tucker, and E.C. Lightowers, *Phys. Rev. B* 60, 12775 (1999).
34. V.P. Markevich and M. Suezawa, *J. Appl. Phys.* 83, 2988 (1998).
35. B. Hourahine, R. Jones, A.N. Safonov, S. Öberg, P.R. Briddon, and S.K. Estreicher, *Phys. Rev. B* 61, 12594 (2000).
36. M. Budde, B. Bech Nielson, P. Leary, J. Goss, R. Jones, P.R. Briddon, S. Öberg, and S.J. Breuer, *Phys. Rev. B* 57, 4397 (1998).
37. C.G. Van de Walle and J. Neugebauer, *Phys. Rev. B* 52, R14320 (1995).
38. B.L. Sopori, K. Jones, and X.J. Deng, *Appl. Phys. Lett.* 61, 2560 (1992).
39. B.L. Sopori, U.S. patent 5,426,061 20 June 1995.
40. P. Balk, *Extended Abs., Electron. Div.; Electrochem. Soc.* 14, 237 (1965).
41. N.M. Johnson, D.K. Biegelsen, and M.D. Moyer, *J. Vac. Sci. Technol.* 19, 390 (1981).
42. B.L. Sopori, M.I. Symko, R. Reedy, K. Jones, and R. Matson, *Proc. IEEE PVSC* (Piscataway, NJ: IEEE, 1997), pp. 25–30.
43. M. Symko (Ph.D. thesis, University of Denver, 1998).
44. W.L. Hansen, S.J. Pearton, and E.E. Haller, *Appl. Phys. Lett.* 44, 606 (1984).
45. N.M. Johnson, *Hydrogen in Semiconductors, Semiconductors and Semimetals*, ed. J.I. Pankove and N.M. Johnson (New York: Academic Press, Inc., 1991), vol. 34, p. 293.
46. S.J. Pearton, *13th Int. Conf. on Defects in Semiconductors*, ed. L.C. Kimerling and J.M. Parsey, Jr. (Warrendale, PA: TMS-AIME), p. 737.
47. N.M. Johnson and M.D. Moyer, *Appl. Phys. Lett.* 46, 787 (1985).
48. A. Mogro-Campero, R.P. Love, and R. Schubert, *J. Electrochem. Soc.* 132, 2006 (1985).
49. N.M. Johnson, C. Herring, and D.J. Chadi, *Phys. Rev. Lett.* 56, 769 (1986).
50. N.M. Johnson and C. Herring, *Inst. Phys. Conf. Ser.* 95, 415 (1989).
51. T. Ichimiya and A. Furuichi, *Int. J. Appl. Rad. Isotopes* 19, 573 (1968).
52. M. Capizzi and A. Mittiga, *Appl. Phys. Lett.* 50, 918 (1987).
53. C.H. Seager and R.A. Anderson, *Appl. Phys. Lett.* 53, 1181 (1988).
54. Y. Zhang, B. Sopori, R. Reedy, K. Jones, and N.M. Ravindra, *11th Workshop on Crystalline Silicon Solar Cell Materials and Processes: Extended Abstracts and Papers from the Workshop*, Estes Park, CO, August 19–22, NREL, Golden, CO, 2001, pp. 279–284.
55. B.Y. Tong, X.W. Wu, G.R. Yang, and S.K. Wong, *Can. J. Phys.* 67, 379 (1989).
56. B.L. Sopori and Y. Zhang (Paper presented at Proc. NCPV Review Meeting, Lakewood, CO, Oct. 14–17, 2001).
57. B.L. Sopori, X. Deng, J.P. Benner, A. Rohatgi, P. Sana, S.K. Estreicher, Y.K. Park, M.A. Roberson, *Solar Energy Mater. Solar Cells* 41/42, 159 (1996).
58. I. Lundstrom, M.S. Shivaraman, and C. Svenson, *J. Appl. Phys.* 46, 3876 (1975).
59. K.L. Brower, *Phys. Rev. B* 38, 9657 (1988).
60. F.B. McLean, *IEEE Trans. Nucl. Sci.* NS-27, 1651 (1980).
61. D.L. Griscom, *J. Electron. Mater.* 21, 763, (1992).
62. T.C. Shen, C. Wang, G.C. Abeln, J.R. Tucker, J.W. Lyding, P. Avouris, and R.E. Walkup, *Science* 268, 1590 (1995).
63. J.W. Lyding, K. Hess, and I.C. Kizilyalli, *Appl. Phys. Lett.* 68, 2526 (1996).
64. I.C. Kizilyalli, J.W. Lyding, and K. Hess, *IEEE Electron Dev. Lett.* 18, 81 (1997).
65. R.A.B. Devine, J.L. Autran, W.L. Warren, K.L. Vanheusdan, and J.C. Rostaing, *Appl. Phys. Lett.* 70, 2999 (1997).
66. J. Lee, Z. Chen, K. Hess, and J.W. Lyding, *Mater. Res. Soc. Symp. Proc.* 510, 310 (1998).
67. P.J. Chen and R.M. Wallace, *Mater. Res. Soc. Symp. Proc.* 513, 325 (1998).
68. I.C. Kizilyalli, G.C. Abeln, Z. Chen, J. Lee, G. Weber, B. Kotzias, S. Chetlur, J.W. Lyding, and K. Hess, *IEEE Electron Dev. Lett.* 19, 444 (1998).
69. J. Lee, K. Cheng, Z. Chen, K. Hess, J.W. Lyding, Y.K. Kim, H.S. Lee, Y.W. Kim, and K.P. Suh, *IEEE Electron Dev. Lett.* 21, 221 (2000).
70. C.G. Van de Walle and W.B. Jackson, *Appl. Phys. Lett.* 69, 2441 (1996).
71. S. Sugiyama, J. Yang, and S. Guha, *Appl. Phys. Lett.* 70, 378 (1997).
72. J.H. Wei, M.S. Sun, and S.C. Lee, *Appl. Phys. Lett.* 71, 1498 (1997).
73. R.A.B. Devine, J.L. Autran, W.L. Warren, K.L. Vanheusdan, and J.C. Rostaing, *Appl. Phys. Lett.* 70, 2999 (1997).